



# JGR Atmospheres

## RESEARCH ARTICLE

10.1029/2018JD030001

### Key Points:

- Uncertainty in assumed effective emission height strongly affects SO<sub>2</sub> concentration and vertical profile
- The impact of emission injection height uncertainty varies by emission species
- Aerosols and their climate impacts can be influenced by emission height

### Supporting Information:

- Supporting Information S1

### Correspondence to:

S. J. Smith and H. Wang,  
ssmith@pnnl.gov;  
hailong.wang@pnnl.gov

### Citation:

Yang, Y., Smith, S. J., Wang, H., Lou, S., & Rasch, P. J. (2019). Impact of anthropogenic emission injection height uncertainty on global sulfur dioxide and aerosol distribution. *Journal of Geophysical Research: Atmospheres*, 124, 4812–4826. <https://doi.org/10.1029/2018JD030001>

Received 16 NOV 2018

Accepted 31 MAR 2019

Accepted article online 13 APR 2019

Published online 30 APR 2019

©2019. American Geophysical Union.  
All Rights Reserved.

Notice: Manuscript authored by Battelle Memorial Institute under contract DE-AC05-76RL01830 with the US Department of Energy. The US Government retains and the publisher, by accepting the article for publication, acknowledges that the US Government retains a nonexclusive, paid-up, irrevocable, worldwide license to publish or reproduce the published form of this manuscript, or allow others to do so, for US Government purposes. The Department of Energy will provide public access to these results of federally sponsored research in accordance with the DOE Public Access Plan: (<http://energy.gov/downloads/doe-public-access-plan>).

## Impact of Anthropogenic Emission Injection Height Uncertainty on Global Sulfur Dioxide and Aerosol Distribution

Yang Yang<sup>1</sup> , Steven J. Smith<sup>2</sup> , Hailong Wang<sup>1</sup> , Sijia Lou<sup>1</sup> , and Philip J. Rasch<sup>1</sup>

<sup>1</sup>Atmospheric Sciences and Global Change Division, Pacific Northwest National Laboratory, Richland, WA, USA, <sup>2</sup>Joint Global Change Research Institute, Pacific Northwest National Laboratory, College Park, Maryland, USA

**Abstract** Anthropogenic sulfur compounds play an important role in acid deposition, aerosol particle formation, and subsequent radiative forcing and human fine particulate exposure. There are substantial uncertainties in processes influencing sulfate and precursor distributions, however, that have not yet been resolved through comparisons with observations. We find here an underappreciated factor that has a large impact on model results: uncertain emission height. Global aerosol-climate model simulations indicate that the assumed effective anthropogenic emission height is very important to SO<sub>2</sub> near-surface concentrations and vertical profile. The global range of near-surface SO<sub>2</sub> concentration over land (ocean) due to uncertainty in industrial (international shipping) emission injection height is 81% (76%), relative to the average concentration. This sensitivity is much larger than the uncertainty of SO<sub>2</sub> emission rates. Black carbon and primary organic matter concentration and profiles are also sensitive to emission heights (53% over land and 28% over oceans). The impact of emission height uncertainty is larger in winter for land-based emissions, but larger in summer over the Northern Hemisphere ocean for shipping emissions. The variation in aerosol optical depth related to shipping emission injection heights is 11% over oceans, revealing the potential importance of injection height on aerosol forcing and climatic effects. The large impact on SO<sub>2</sub> concentrations can confound attempts to use surface, aircraft, and satellite observations to constrain the importance of other processes that govern sulfur compound distributions in the atmosphere. The influence of emission height on vertical SO<sub>2</sub> column also will impact the accuracy of satellite retrievals.

**Plain Language Summary** Models are central tools in understanding how air pollutants are transported and transformed within the atmosphere, and it is essential to evaluate modeled air pollutants by comparing to observations. The conversion of sulfur dioxide to sulfate aerosol in the atmosphere is important for both climate forcing and air pollution analysis. We find that modeled near-surface concentration and vertical distribution of sulfur dioxide gas are very sensitive to the assumed effective emission height, with the influence of injection height differing by season and region. The uncertainty in assumed effective emission height can also affect aerosol radiative forcing and its climatic effects. Given that emission heights are uncertain, the ability to evaluate the sulfur cycle and aerosol forcing in models may be compromised.

## 1. Introduction

Emission data are an essential input for both climate and chemical transport models. Regional and temporal emission variations can significantly affect modeled concentrations, long-range transport and lifetime of gases and particles, and potentially their climate impacts (Pegger & Friedrich, 2009; Sofiev et al., 2013). Previous studies have reported a large variation between modeled column burdens and lifetimes of SO<sub>2</sub> gas and aerosols, including sulfate, black carbon (BC), and primary organic matter (POM), between models (Roelofs et al., 2001; Textor et al., 2006). It is important to reduce uncertainties in modeling sulfur chemistry, particularly the conversion of gaseous SO<sub>2</sub> to particulate sulfate aerosols, given the large role sulfate aerosols play in acid deposition, radiative forcing, and human health exposure. SO<sub>2</sub> in situ measurements are generally available only at the surface. Errors in surface concentrations result from a combination of biases in emission strength or spatial distribution, model parameterizations, and, as we quantify here, emission injection height.

The height at which an emission species is injected into the atmosphere would be expected to impact transport, lifetime, and interactions with other atmospheric constituents. Assumptions about the injection height of emissions might, therefore, impact both model results and observables in the real world. Indeed, tall emission stacks were introduced over the last century in order to reduce local impacts of harmful air pollutants, but while that reduces surface concentrations, it does not affect the total sulfur release. Many studies have identified injection heights of open biomass burning and volcanic emissions to be important factors influencing tracer gas and aerosols (Ge et al., 2016; Jian & Fu, 2014; Luderer et al., 2006). However, open burning studies focus on primary aerosol emissions, and the issue of emission height is of an entirely different magnitude for major volcanic eruptions (e.g., stratospheric injection). SO<sub>2</sub> is an aerosol precursor, and an important source for secondary formation of sulfate aerosols, that is formed in minutes to tens of days downstream of the emission source (depending on altitude and oxidation pathway). The appropriate injection height to use for anthropogenic emissions in global models is still unclear, and the influence of the uncertainty in injection height of anthropogenic emissions on modeled values needs quantification. A few regional modeling studies have examined the impact of injection heights of anthropogenic emissions (Akingunola et al., 2018; de Meij et al., 2006; Mailler et al., 2013), but this factor is rarely mentioned in the global aerosol modeling literature.

Pozzer et al. (2009) conducted a pair of simulations in a global atmospheric chemistry model, one simulation with anthropogenic and biomass burning emissions released in the lowest model layer and another one applying height dependent emissions. They found a strong sensitivity of vertical distribution for NO<sub>x</sub>, CO, nonmethane hydrocarbons, and O<sub>3</sub>, but they did not examine SO<sub>2</sub>, which can be more sensitive to emission injection height (Bieser et al., 2011). Using a nested global chemical transport model and two set of European emission data, de Meij et al. (2006) reported a large difference in modeled SO<sub>2</sub> near-surface concentrations by a factor of 2 due to different emission injection height, but they only focused on Europe. Mailler et al. (2013) performed simulations with different emission heights using a regional chemical transport model, also focusing on Europe, and found that applying European vertical emissions profiles from the plume rise model of Bieser et al. (2011) significantly reduced model biases in simulated SO<sub>2</sub> and NO<sub>2</sub> concentrations compared to observations. We focus in this work on quantifying, for the first time to our knowledge, the global impact of the uncertainty in anthropogenic emission injection height on SO<sub>2</sub> and aerosols.

Power plant and some industrial emissions, as well as emissions from international shipping, generally result in a high temperature exhaust that rises in a buoyant plume, although this behavior is also affected by ambient temperature and wind speed, as well as other meteorological conditions such as inversion layers. An accurate estimate of the effective injection height therefore requires information on stack height, exhaust temperature, and velocity, along with meteorological conditions (Pegger & Friedrich, 2009). Plume rise, together with variable stack height, leads to a large uncertainty in the effective injection height. Using effective emission heights from plume rise calculations can reproduce tracer concentrations in air quality models (Guevara et al., 2014), but this technique has not been applied in global models. Note that because of the dependence on meteorological conditions, plume height is not constant for any emission source but varies within a certain range, for example, observed to be roughly  $\pm 50\%$  in Akingunola et al. (2018) for a large oil sands source. The combination of stack height plus plume rise can be considered an effective emission height, simplified to emission height hereafter.

Due to a lack of detailed emission height data, many global chemistry-climate models depend on exogenous assumptions for injection heights of anthropogenic emissions (Hurrell et al., 2013; Stier et al., 2005). In the AeroCom (Aerosol Comparisons between Observations and Models) protocols (Dentener et al., 2006), industrial and power plant emissions are injected evenly between 100 and 300 m above the surface. However, this injection height relies on expert judgment (de Meij et al., 2006), and the measured plume rise can reach an altitude much higher than 300 m (Gordon et al., 2017), even exceeding 1,000 m for large source complexes in some conditions (Akingunola et al., 2018). International shipping emissions are generally assumed to be injected into the lowest model layer, such as in the AeroCom protocols, but they can also be injected into higher altitudes (Stier et al., 2005). Many global models have surface layers that are around 100-m thick, which means that assuming injection into the lowest model layer may not be appropriate. Applying a standard injection height assumption in models without quantifying the uncertainty associated with the assumption may result in misinterpretation of surface concentration discrepancies between models and

measurements. Although this problem is in principle known in the modeling community, the quantitative impact of this uncertainty has not been assessed and many modeling studies on aerosol distribution and radiative effects do not take this into consideration (Myhre et al., 2013; Tsigaridis et al., 2014).

In this study, we examine the impact of the uncertainty in injection heights of anthropogenic emissions in the Community Atmosphere Model version 5 (CAM5), an aerosol-climate model, equipped with an aerosol source tagging technique. We quantify the spatial and temporal ranges of modeled near-surface concentrations of SO<sub>2</sub> gas (sulfur dioxide and precursor of sulfate), and aerosols of sulfate, BC, and POM due to the uncertainty in industrial sector emission height. Otherwise noted, the results in this study are based on near-surface concentrations. We focus on the industrial sector because of the heterogeneity of emission sources in this sector implies a large uncertainty in the effective injection height. Our insights, however, also apply to energy sector emissions. In addition, international shipping emissions over ocean are also analyzed given the generally different atmospheric conditions over ocean areas.

## 2. Methods

A 10-year simulation between 2005 and 2014, after 1-year spin-up, has been conducted with time varying emissions and meteorological conditions using CAM5. The model can simulate precursor gases and aerosols including SO<sub>2</sub>, sulfate, BC, POM, secondary organic aerosol, sea salt, and dust (Liu et al., 2012). In addition to model modifications resulting in improved convective transport and aerosol wet scavenging (Wang et al., 2013), wind fields are nudged to the MERRA (Modern Era Retrospective-Analysis for Research and Applications) reanalysis (Rienecker et al., 2011) version 5.2.0 to minimize the impact of potential model biases on the transport of gases and aerosols. The simulation is performed at a horizontal grid of 1.9° latitude × 2.5° longitude with 30 vertical layers from the surface to 3.6 hPa. The CEDS (Community Emissions Data System) anthropogenic precursor gases and aerosol emissions (version 2017-05-18, Hoesly et al., 2018) obtained from the CMIP6 (Coupled Model Intercomparison Project Phase 6) data sets are used in this study. Open biomass burning emissions are from van Marle et al. (2017). Natural volcanic and dimethyl sulfide emissions are from AeroCom following Hurrell et al. (2013), which are kept at a present-day climatological mean level. The CAM5 model performance in simulating SO<sub>2</sub> gas and aerosols has been evaluated against surface measurements and satellite retrievals in many previous studies (Yang, Wang, Smith, Ma, et al., 2017; Yang, Wang, Smith, Easter, et al., 2017; Yang, Wang, Smith, Easter, & Rasch, 2018; Yang, Wang, Smith, Zhang, Lou, Qian, et al., 2018; Yang, Wang, Smith, Zhang, Lou, Yu, et al., 2018). In general, the model can well reproduce aerosols in less polluted source regions like Europe and North America but underestimates aerosol concentrations in polluted source regions like East Asia and has large uncertainties over remote regions.

An aerosol source tagging capability is implemented in CAM5, which explicitly tags and tracks emission, evolution, transport, and removal of aerosols and their precursor gases with only one simulation. This technique has been previously used to examine source-receptor relationships of aerosols globally and regionally (Yang, Wang, Smith, Easter, et al., 2017; Yang, Wang, Smith, Ma, & Rasch, 2017; Yang, Wang, Smith, Easter, & Rasch, 2018; Yang, Wang, Smith, Zhang, Lou, Qian, et al., 2018). In standard CAM5, SO<sub>2</sub> from industry and energy sector is evenly emitted at 100–300 m above the surface, with 76% of which is emitted into the second model layer above the surface, 13% into the bottom layer and 11% into the third model layer. Other anthropogenic sectors, including international shipping, are emitted from the surface (into the lowest model layer) following AeroCom protocols. All anthropogenic sectors of BC and POM are emitted from the surface.

To examine the influence of different injection heights on aerosol modeling, emissions from the CEDS industry sector (see Text S1 and Table S1 in the supporting information) are redistributed into the lowest four layers of the model. The center altitudes of these four layers are around 63, 202, 366, and 554 m above the surface and the top altitudes are at 126, 278, 454, and 654 m, which span most of the range of observed injection heights (Carson & Moses, 1969). While injection heights are higher than the fourth model layer (from the surface) in some instances, these seem likely to be atypical cases. A quarter (25%) of industrial sector emissions are injected into each of the four layers, which are separately tagged. For analysis purposes, the simulated gas and aerosol concentrations in each tagged layer are multiplied by 4 as if 100% of industrial emissions were injected into the same layer (hereafter, IND1, IND2, IND3, and IND4 corresponding to

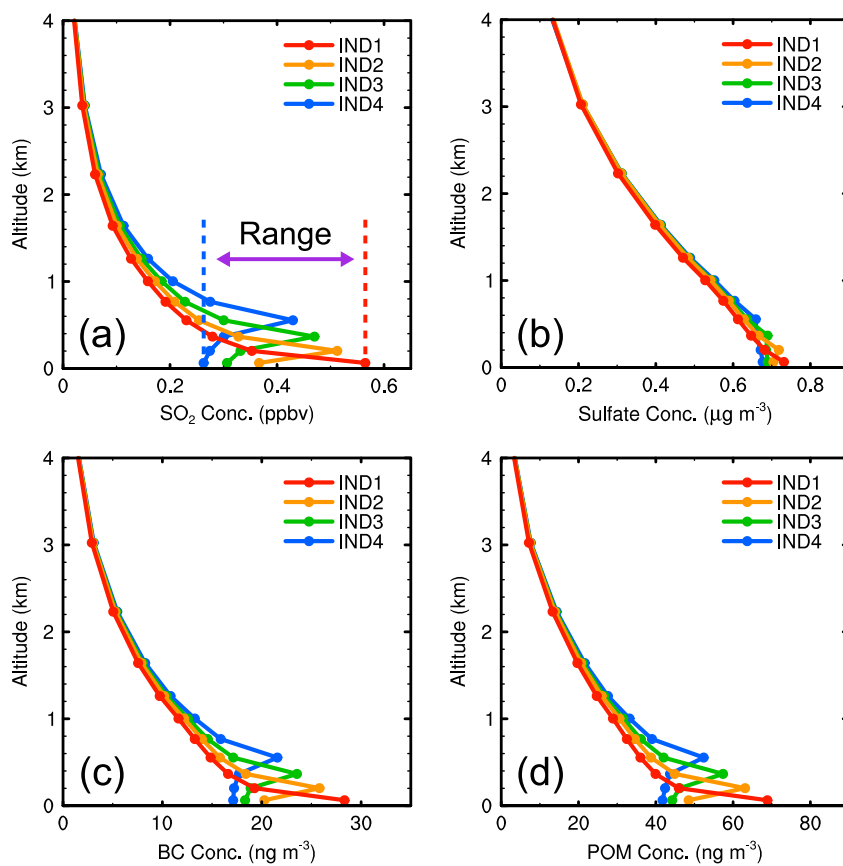


**Figure 1.** Global mean vertical profiles of concentrations of (a) SO<sub>2</sub> (ppbv), (b) sulfate (ng/m<sup>3</sup>), (c) black carbon (BC; ng/m<sup>3</sup>), and (d) primary organic matter (POM; ng/m<sup>3</sup>) over land contributed by industrial emissions injected into model layers 1 to 4 (IND1, IND2, IND3, and IND4).

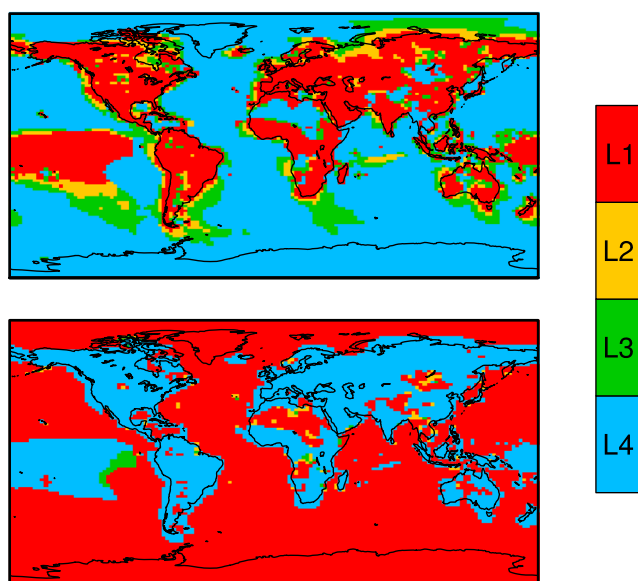


**Figure 2.** Model layer that injected industrial SO<sub>2</sub> emissions produces maximum (top) and minimum (bottom) of near-surface SO<sub>2</sub> concentrations from model layer 1 (L1) to layer 4 (L4).

the four tags). In two test simulations in which 100% and 20% of industrial emissions were emitted, respectively, using the same injection assumption, we find that the difference of SO<sub>2</sub> and sulfate concentrations from 100% emission and 20% emission multiplied by 5 are within 5% (Figure S1), which is likely due to changes in lifetime. In addition to the four tags for industrial emissions (IND1-4), another four tags are assigned to international shipping emissions (SHP1-4) with a similar emission injection strategy (i.e., 25% injected to each of the lowest four model layers). IND1-4 and SHP1-4 are from the same simulation but analyzed separately.

### 3. Results

Figure 1a shows the global average vertical profile for SO<sub>2</sub> over land from industrial sector emissions emitted into the first four model layers. Upon emission in the atmosphere, SO<sub>2</sub> is vertically redistributed by turbulence and convective mixing in the model, resulting in vertical dilution. SO<sub>2</sub> injection into the lowest model layer (IND1) gives the highest SO<sub>2</sub> concentrations near the surface, which monotonically decreases with height. Injection into higher layers results in a concentration peak in that layer and the peak concentrations also decrease with height. This is because 25% amount of industrial emission is emitted in each of model layers

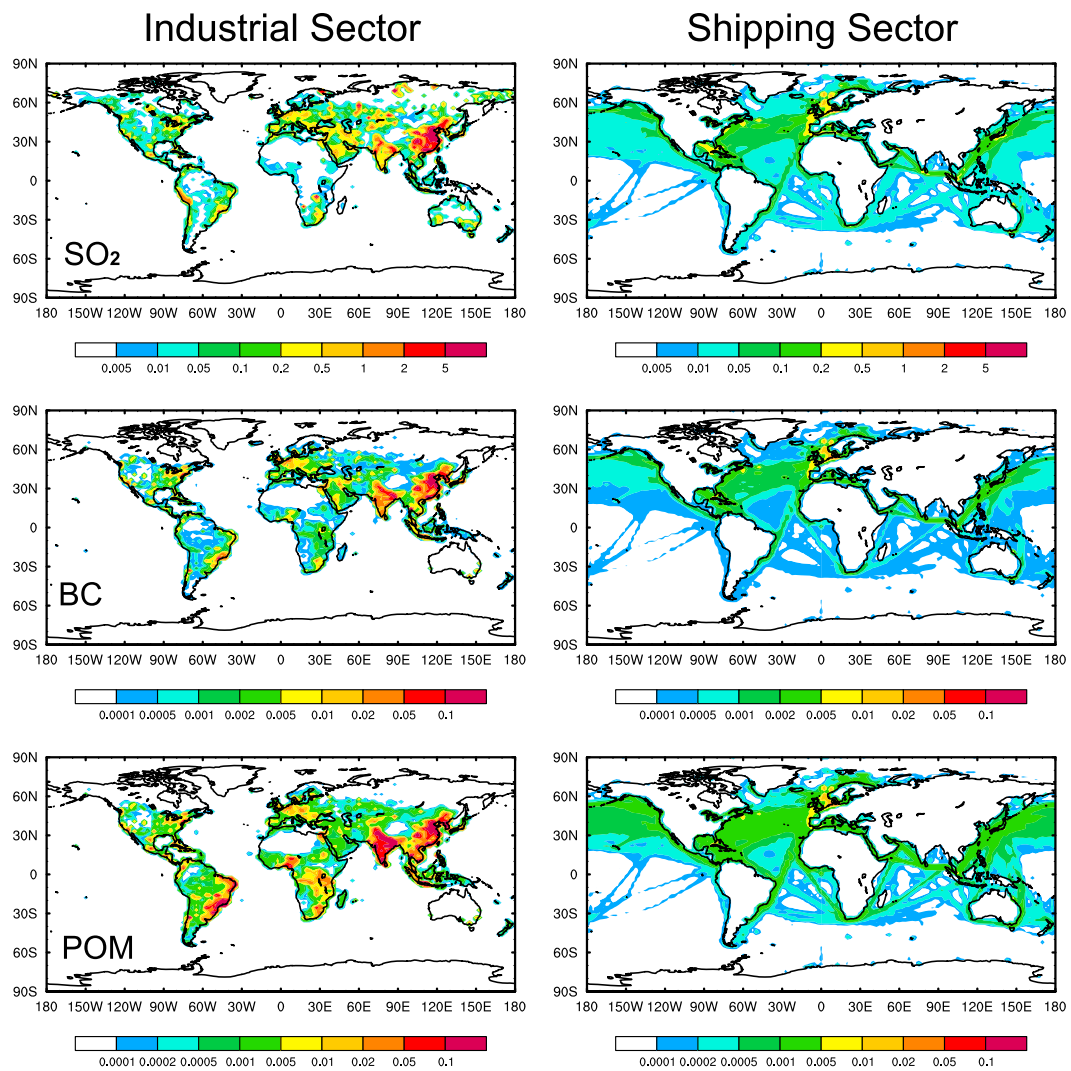


**Figure 3.** Spatial distribution of annual mean SO<sub>2</sub> (top row), black carbon (BC; middle row), and primary organic matter (POM; bottom row) emissions ( $\text{g m}^{-2} \text{yr}^{-1}$ ) from industrial (left column) and shipping (right column) sectors averaged over 2005–2014.

1–4. With larger layer thickness (larger volume) from model layers 1–4, the peak concentration decreases. As a result, both SO<sub>2</sub> surface concentrations and SO<sub>2</sub> vertical profiles change substantially depending on injection height. This diversity in vertical SO<sub>2</sub> concentration is reflected in in situ aircraft measurements over China (He et al., 2012), which showed a variety of vertical profiles from monotonically decreasing with height to profiles with peaks at various altitudes. In a test simulation, the vertical profile of SO<sub>2</sub> using model default industrial emission height is almost the same as IND2 in Figure 1, since that 76% of industrial SO<sub>2</sub> emissions are injected in model layer 2 in the default emission assumptions.

However, the secondary aerosol-sulfate shows very small differences as injection height changes compared to SO<sub>2</sub> gas (Figure 1b). This is also reported by Guevara et al. (2014) using a regional model, in which they found that using fixed or bottom-up calculated emission injection heights can cause a 20%–30% difference in modeled SO<sub>2</sub> concentrations in Europe but a negligible influence on sulfate. This is because, after formation from gas phase and aqueous phase oxidation of SO<sub>2</sub>, sulfate experiences redistribution by vertical mixing, leading to a lower impact of the initial injection height compared to the dynamical impact.

Primary aerosols, BC and POM, show larger changes in surface concentrations and vertical profiles than sulfate but smaller than SO<sub>2</sub> gas. This results from the longer lifetime of aerosols than SO<sub>2</sub> gas, leading to a more

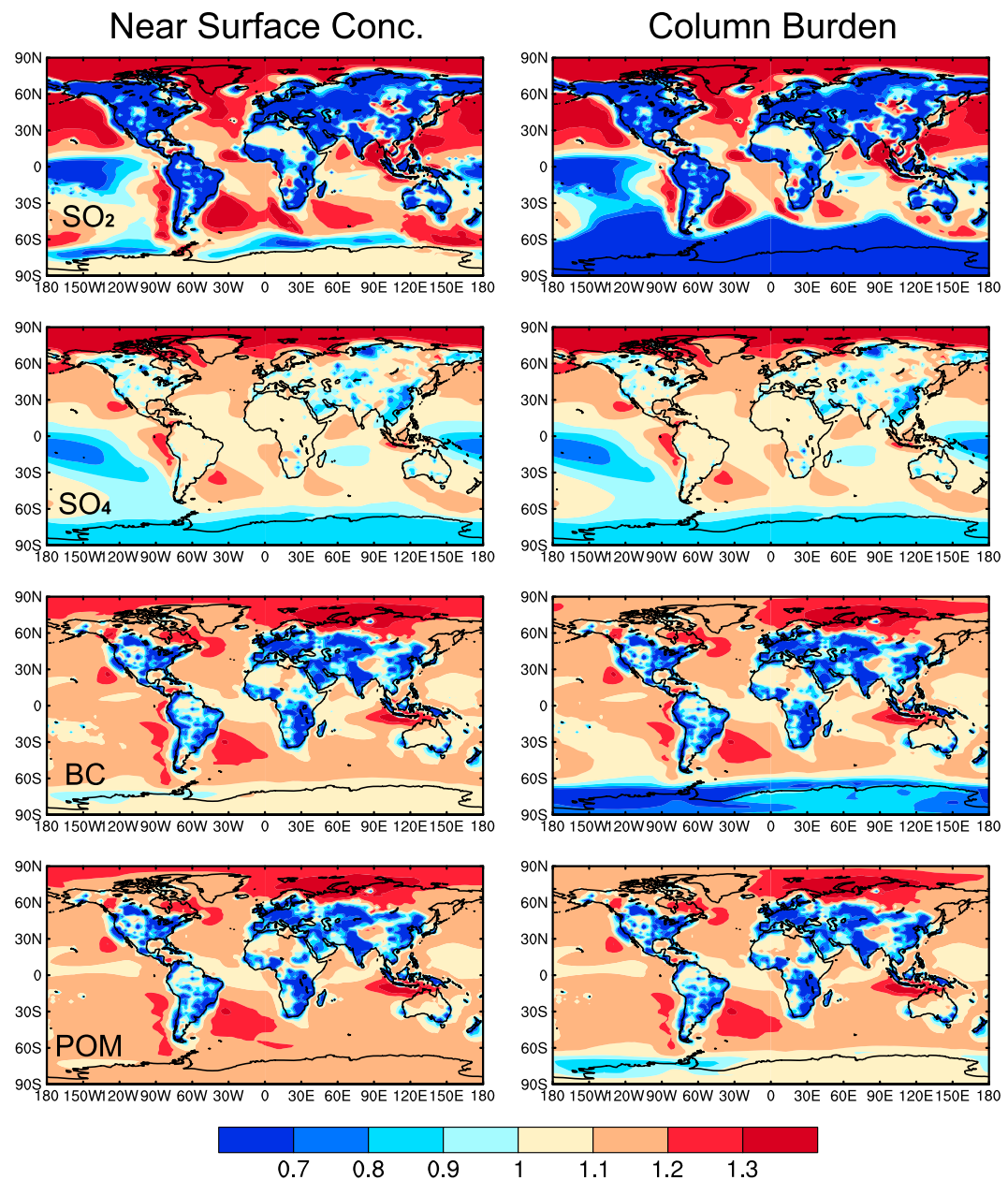


**Figure 4.** Ratios of near-surface concentration (left column) and column burden (right column) of  $\text{SO}_2$ , sulfate, black carbon (BC), and primary organic matter (POM; from top to bottom) between IND4 and IND1 (IND4/IND1).

important role of mixing on aerosol vertical distributions and, therefore, reducing the impact of emission height assumptions. This finding is consistent with Jian and Fu (2014) who note that pollutants with relatively long lifetimes are insensitive to injection heights.

We define the range of near-surface concentrations due to injection height uncertainty as the difference between maximum and minimum of near-surface concentrations from the four IND tags (IND1-4). Most of land regions have a maximum near-surface  $\text{SO}_2$  concentration with IND1 injection, while maximum near-surface  $\text{SO}_2$  concentration from industrial emission over oceans is found with IND4 injection (Figure 2), because of the elevated transport of  $\text{SO}_2$  from polluted land regions to oceans. Over land regions with relatively low local emissions (Figure 3), the maximum near-surface  $\text{SO}_2$  concentration is also found in tags with injection height above the bottom layer due to transport of  $\text{SO}_2$  from neighboring high emission

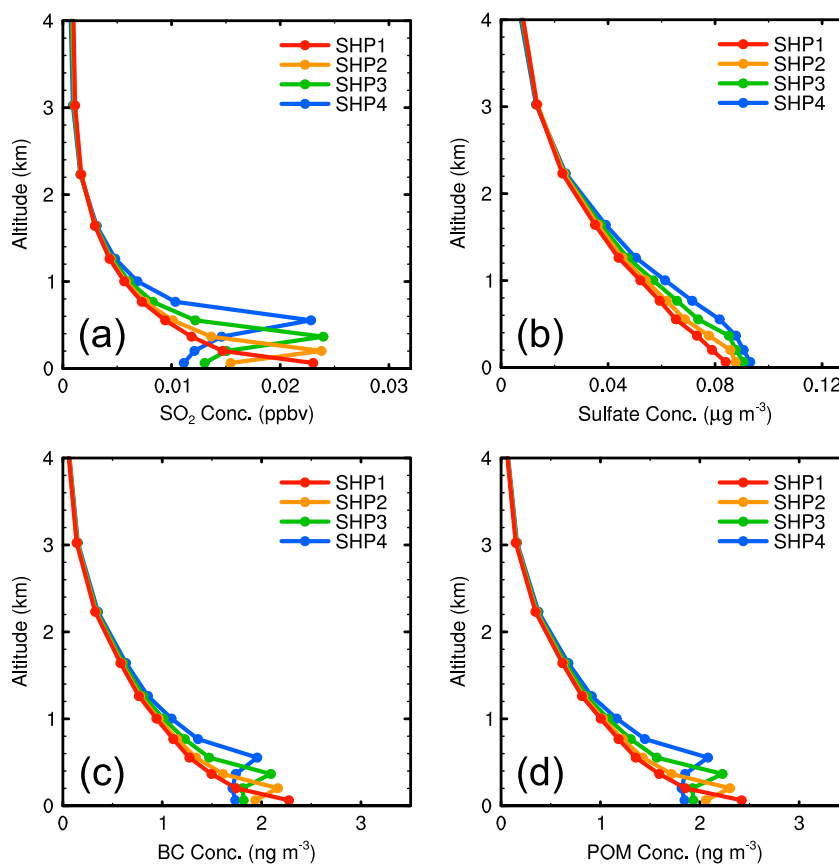


**Figure 5.** Global mean vertical profiles of concentrations of (a) SO<sub>2</sub> (ppbv), (b) sulfate (ng/m<sup>3</sup>), (c) black carbon (BC; ng/m<sup>3</sup>), and (d) primary organic matter (POM; ng/m<sup>3</sup>) over oceans contributed by international shipping emissions injected into layer 1 to 4 (SHP1, SHP2, SHP3, and SHP4).

regions. The global annual mean range of near-surface SO<sub>2</sub> concentration over land due to uncertainty in industrial emission injection height during the analyzed 10 years is 0.30 ppbv (parts per billion by volume; Figure 1a), which is 81% relative to the average of IND1-4, (referred to as relative range hereafter), whereas the range of sulfate aerosol is 0.06 μg/m<sup>3</sup>, only 8% relative to the average. The relative range of SO<sub>2</sub> due to uncertainty in emission injection height is much larger than the uncertainty of SO<sub>2</sub> emission rates (8–14% globally; Smith et al., 2011) on modeled SO<sub>2</sub> near-surface concentrations. BC and POM show the same relative range of 53% over land globally since they are often coemitted and share many common physical tendencies in this model.

Uncertainty in emission injection height can also affect long-range transport over oceans, which is important to both air quality in remote regions and aerosol radiative forcing over dark oceans. Higher industrial emission height produces larger near-surface concentration and column burden of aerosols over midlatitude oceans, with values from IND4 being 10%–20% higher than those from IND1 (Figure 4).

The global average vertical profile for SO<sub>2</sub> over oceans from international shipping emissions (Figure 5) shows a similar type of impact on surface concentrations as land-based emissions; however, the peak SO<sub>2</sub> concentration does not decrease so strongly, or even increases, with injection height. This behavior is likely because of in-cloud aqueous phase oxidation of SO<sub>2</sub> around model layers 2–3, leading to a shorter SO<sub>2</sub> lifetime and hence a larger importance of initial injection height. The relative ranges due to shipping injection height uncertainty are also similar to those of industrial sector for SO<sub>2</sub> and sulfate, with values of 76% and 10%, respectively. The relative range of both BC and POM near-surface concentrations due to shipping injection height uncertainty is 28%, lower than the range of 53% due to industrial sector injection height uncertainty, probably resulting from stronger turbulence and convective mixing over ocean than land.

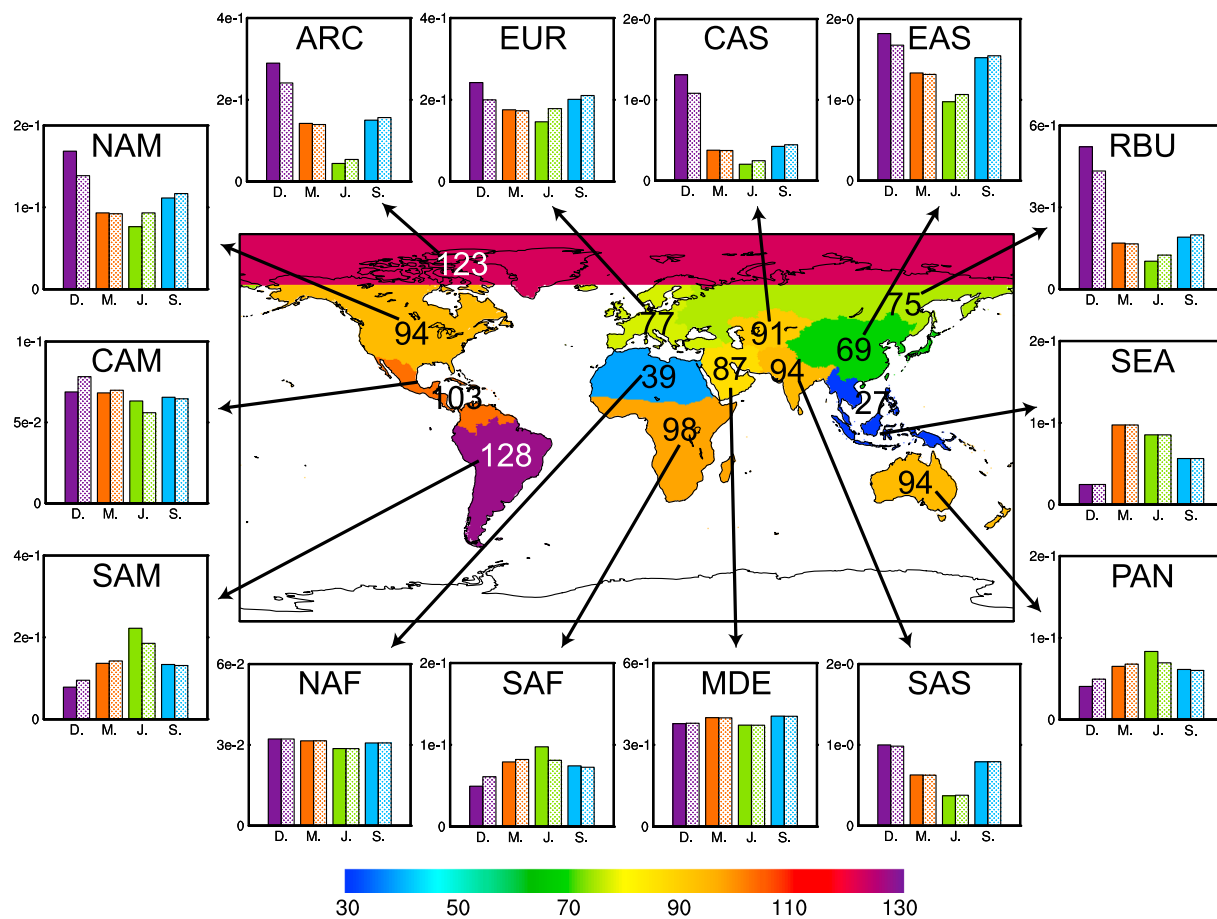


**Figure 6.** Annual mean relative range (%, inside spatial map) of near-surface  $\text{SO}_2$  concentrations due to the uncertainty in injection heights of industrial emissions in 14 regions over land, including the Arctic (ARC), Europe (EUR), Central Asia (CAS), East Asia (EAS), Russia/Belarus/Ukraine (RBU, hereafter Russia), Southeast Asia (SEA), Pacific/Australia/New Zealand (PAN, hereafter Australia), South Asia (SAS), the Middle East (MDE), Southern Africa (SAF), North Africa (NAF), South America (SAM), Central America (CAM), and North America (NAM). Outside are seasonal mean range (ppbv, solid bars) and normalized range (ppbv, dotted bars) in December-January-February (D.), March-April-May (M.), June-July-August (J.), and September-October-November (S.) for the fourteen regions.

Figure 6 shows a spatial map of modeled annual mean relative range of industrial near-surface  $\text{SO}_2$  concentrations due to the uncertainty in injection heights in fourteen regions over land. Over regions with relatively weak emission (Figure 3), due to higher near-surface  $\text{SO}_2$  concentrations from nonlocal contributions with injection heights (IND2-4) above bottom layer (IND1), the regional average of relative range is lower (e.g., North Africa and Southeast Asia). In many of the regions, industrial emission injection height uncertainty leads to a relative range of 70%–130%. There is a high relative range of 123% in the Arctic because near-surface  $\text{SO}_2$  is largely influenced by industrial emissions transported from lower-latitude regions when emissions have an elevated injection height (Yang, Wang, Smith, Easter, & Rasch, 2018). The maximum concentration over most of the Arctic, therefore, results from injection of distant emissions into the IND4 layer. The relative range in Europe is 77% in this study, similar to 50%–100% shown in Mailler et al. (2013).

Yang, Wang, Smith, Easter, et al. (2017) reported a discrepancy of 25%–45% between modeled and measured near-surface  $\text{SO}_2$  concentration in East Asia. However, the different injection heights can cause a 69% uncertainty in the modeled value, much higher than the discrepancy between the model and measurements.

In terms of the absolute values (Table 1), East Asia has the largest range of near-surface  $\text{SO}_2$  concentration due to the industrial emission height uncertainty, with an annual mean of 1.42 ppbv, followed by 0.71 ppbv in South Asia and 0.57 ppbv in Central Asia, due to high  $\text{SO}_2$  emissions from industrial activities. The Middle East and Russia show an absolute range of 0.39 and 0.24 ppbv, respectively, while ranges in other regions are lower than 0.20 ppbv. The ranges show different seasonality over different regions driven by changes in

**Table 1**

Annual (ANN) and Seasonal Mean Model and Normalized Range of SO<sub>2</sub> (ppbv) Due to the Uncertainty in Injection Heights of Industrial Emissions Over 14 Regions of the Globe, Including North America (NAM), Central America (CAM), South America (SAM), Europe (EUR), North Africa (NAF), Southern Africa (SAF), the Middle East (MDE), Southeast Asia (SEA), Central Asia (CAS), South Asia (SAS), East Asia (EAS), Russia/Belarus/Ukraine (RBU, Hereafter Russia), Pacific/Australia/New Zealand (PAN, hereafter Australia), and Arctic (ARC), in December-January-February (DJF), March-April-May (MAM), June-July-August (JJA), and September-October-November (SON)

Season	Modeled Range (ppbv)						
	NAM	CAM	SAM	EUR	NAF	SAF	MDE
DJF	0.169	0.069	0.078	0.242	0.032	0.049	0.378
MAM	0.093	0.068	0.137	0.176	0.032	0.079	0.400
JJA	0.076	0.063	0.222	0.146	0.029	0.098	0.372
SON	0.111	0.066	0.134	0.201	0.031	0.074	0.405
ANN	0.111	0.067	0.143	0.190	0.031	0.075	0.390
	SEA	CAS	SAS	EAS	RBU	PAN	ARC
DJF	0.025	1.310	1.000	1.820	0.522	0.041	0.290
MAM	0.097	0.378	0.629	1.333	0.169	0.065	0.142
JJA	0.085	0.205	0.371	0.977	0.102	0.083	0.044
SON	0.056	0.425	0.791	1.521	0.191	0.061	0.150
ANN	0.057	0.573	0.701	1.417	0.244	0.063	0.156
Season	Normalized Range (ppbv)						
	NAM	CAM	SAM	EUR	NAF	SAF	MDE
DJF	0.139	0.078	0.095	0.200	0.032	0.061	0.379
MAM	0.092	0.070	0.142	0.173	0.032	0.082	0.399
JJA	0.093	0.056	0.185	0.178	0.029	0.081	0.372
SON	0.117	0.065	0.131	0.211	0.031	0.073	0.405
ANN	0.111	0.067	0.143	0.190	0.031	0.075	0.390
	SEA	CAS	SAS	EAS	RBU	PAN	ARC
DJF	0.025	1.082	0.985	1.676	0.433	0.050	0.241
MAM	0.097	0.374	0.626	1.315	0.166	0.068	0.140
JJA	0.085	0.248	0.378	1.067	0.125	0.070	0.054
SON	0.056	0.445	0.793	1.545	0.199	0.060	0.157
ANN	0.057	0.573	0.701	1.417	0.244	0.063	0.156

seasonal emission amount and meteorology. In the Northern Hemisphere, the ranges are typically highest in boreal winter and lowest in boreal summer, and the opposite occurs over regions in the Southern Hemisphere (Figure 6).

To separate out the role of meteorological variability from emission seasonality, we normalize the seasonal industrial near-surface SO<sub>2</sub> concentrations by corresponding emissions. Then the normalized range is calculated as the range of normalized concentrations. Most of the normalized ranges present decreases of peaks in the cold season and increases of troughs in the warm season as compared to the absolute model ranges (Figure 6). It suggests that higher (lower) industrial SO<sub>2</sub> emissions in the cold (warm) season can partly explain the seasonal contrast in model ranges. We note that the seasonality for industrial emissions is relatively high in the data set used in this study (<https://github.com/JGCRI/CEDS/issues/8>). Although removing emission seasonality mitigates the seasonal range contrast, the seasonal patterns of normalized ranges do not change for most regions (normalized ranges still peak in the cold season), implying that changes in meteorology are the main driver of the seasonal changes in ranges. Weaker sunlight and lower temperature in the cold season do not favor sulfate formation from SO<sub>2</sub>, resulting in higher SO<sub>2</sub> concentration per unit SO<sub>2</sub> emission and, therefore, higher ranges due to uncertainty in injection height of industrial emissions, and vice versa for the warm season.

For the injection height uncertainty of shipping emissions over ocean (Figure 7), relative ranges of near-surface SO<sub>2</sub> concentration over North Pacific and North Atlantic are within 79%–84%, while smaller over South Pacific, South Atlantic, and Indian Ocean (around 59%–72%), probably due to stronger winds and dynamical impact over the Southern Hemisphere oceans compared to the Northern Hemisphere. The

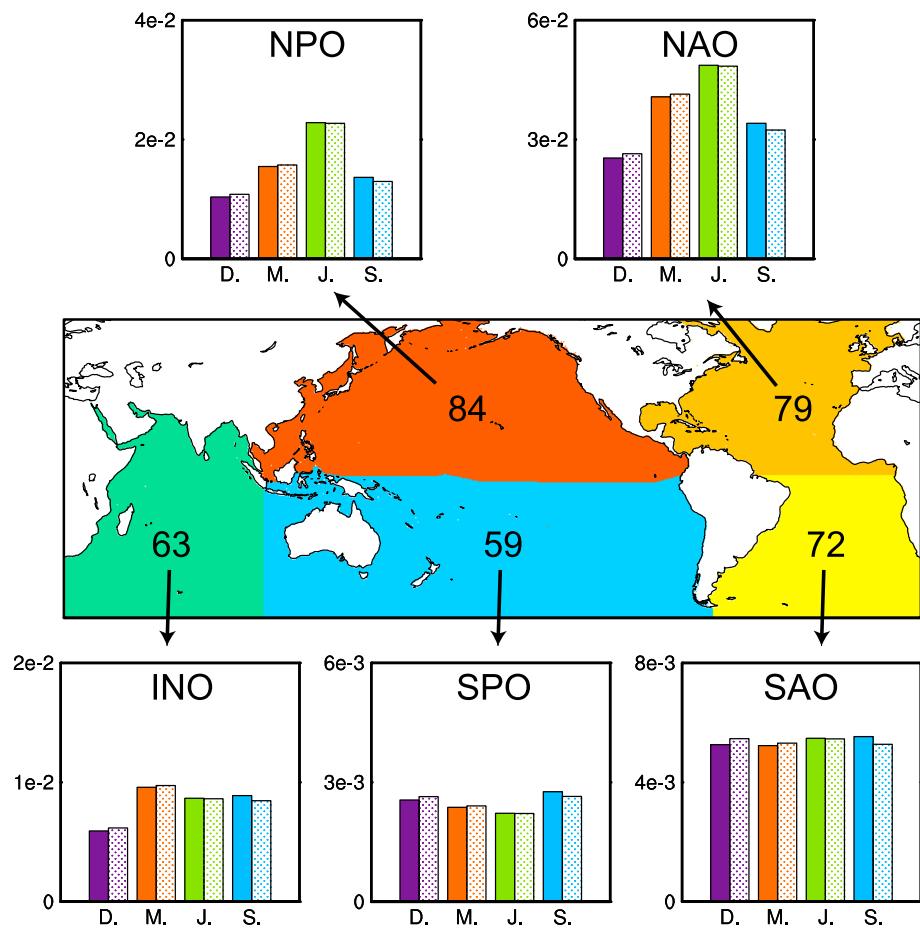


**Figure 7.** Annual mean relative range (%) of near-surface  $\text{SO}_2$  concentrations due to the uncertainty in injection heights of international shipping emissions over oceans, including North Atlantic Ocean (NAO), South Atlantic Ocean (SAO), North Pacific Ocean (NPO), South Pacific Ocean (SPO), and Indian Ocean (INO). Outside are seasonal mean range (ppbv, solid bars) and normalized range (ppbv, dotted bars).

**Table 2**

Annual (ANN) and Seasonal Mean Modeled and Normalized Range of  $\text{SO}_2$  (ppbv) Due to the Uncertainty in Injection Heights of Shipping Emissions Over North Atlantic Ocean (NAO), South Atlantic Ocean (SAO), North Pacific Ocean (NPO), South Pacific Ocean (SPO), and Indian Ocean (INO)

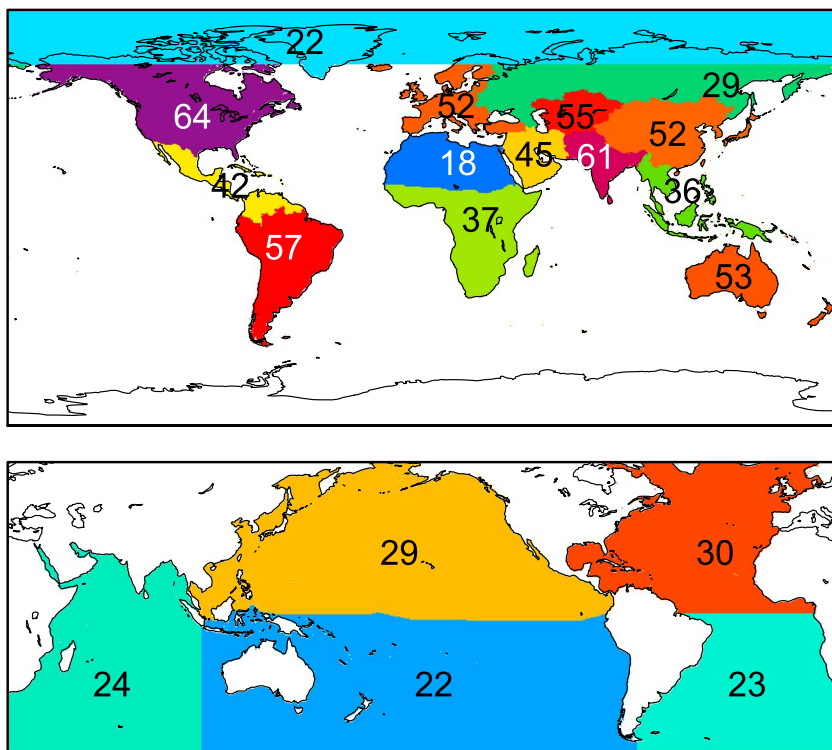
Season	Modeled Range (ppbv)				
	NAO	SAO	NPO	SPO	INO
DJF	0.025	0.005	0.010	0.003	0.006
MAM	0.041	0.005	0.015	0.002	0.010
JJA	0.049	0.005	0.023	0.002	0.009
SON	0.034	0.006	0.014	0.003	0.009
ANN	0.037	0.005	0.016	0.002	0.008

Season	Normalized Range (ppbv)				
	NAO	SAO	NPO	SPO	INO
DJF	0.026	0.005	0.011	0.003	0.006
MAM	0.041	0.005	0.016	0.002	0.010
JJA	0.048	0.005	0.023	0.002	0.009
SON	0.032	0.005	0.013	0.003	0.008
ANN	0.037	0.005	0.016	0.002	0.008

model and normalized ranges are higher in the warm season over the Northern Hemisphere oceans, which is different from the seasonal comparison for industrial sector over land (Figure 6 and Table 2). For example, averaged over North Pacific, range of  $\text{SO}_2$  in June-July-August (JJA) is more than twice as that in December-January-February (DJF). This is partly due to the higher (lower) shipping  $\text{SO}_2$  concentration below (above) the boundary layer in JJA than in DJF (Figure S2), associated with the seasonal shift of downdraft/inversion around  $30^\circ\text{N}$  of the Hadley Cell. In JJA, the downdraft shifts north where more shipping emission located, leading to more  $\text{SO}_2$  within the boundary layer. Ranges for the Southern Hemisphere oceans do not have a strong seasonality because most of shipping emissions in the Southern Hemisphere are between  $0^\circ$  and  $30^\circ\text{S}$ , where seasonal variations of sunlight and temperature are relative weak compared to the high latitudes. The similar seasonality between model and normalized ranges indicates that changes in meteorology dominate the seasonal variation of ranges due to emission injection height uncertainty.

Figure 8 presents the regional relative range of industrial (shipping) near-surface BC concentration over land (ocean) for comparison with those of



**Figure 8.** Annual mean relative range (%) of near-surface black carbon concentrations due to the uncertainty in injection heights of industrial (top) and international shipping (bottom) emissions.

$\text{SO}_2$ . Relative ranges of BC due to uncertainties in injection heights of industrial and shipping emissions show similar spatial patterns but lower values compared to  $\text{SO}_2$ . Over land, relative ranges of industrial BC are between 30% and 65%, except for North Africa, while relative ranges of shipping BC are within 20%–30%.

Table S2 (Table S3) summarizes annual and seasonal model and normalized ranges of near-surface BC concentration due to uncertainty in injection heights of industrial (shipping) emissions over land (ocean), respectively. Ranges of BC due to industrial emission injection height uncertainty over land peak in the cold season and drop in the warm season, similar to the seasonality of  $\text{SO}_2$ . Higher BC emission rates in the cold season explain the decrease in peak and increase in trough of the normalized range, compared to the model range. Both model and normalized ranges of BC due to shipping emission injection height uncertainty over Northern Hemisphere oceans peak in JJA, confirming the meteorological influence on the range seasonality over ocean.

Figure 9 shows differences in annual mean ranges of  $\text{SO}_2$  and BC near-surface concentrations due to the uncertainties in injection heights of industrial and shipping emissions between 2005–2009 and 2010–2014. Tables 3 and S4 summarize these values. The ranges of industrial near-surface  $\text{SO}_2$  concentration increased 21% and 9%, respectively, over East Asia and South Asia from 2005–2009 to 2010–2014, while ranges of industrial BC increased 8% and 27% over these two regions. These are mainly due to the increases in emissions from the industrial sector (Hoesly et al., 2018; Yang, Wang, Smith, Zhang, Lou, Qian, et al., 2018). It indicates that the uncertainty in industrial sector emission injection height becomes increasingly important over East Asia and South Asia. Note that the changes in range are highly related to emission changes. Different emission inventories may produce different results, especially in East Asia where satellite data showed significant decreases in  $\text{SO}_2$  since 2011 (Li et al., 2017). Ranges of industrial  $\text{SO}_2$  decreased over Central Asia, North America, Europe, and Russia, which is also related to the decreases in industrial  $\text{SO}_2$  emissions over these regions. Changes in shipping emissions lead to a decrease in ranges of shipping  $\text{SO}_2$  and BC by about 10%–20% over the Northern Hemisphere oceans during 2005–2014.

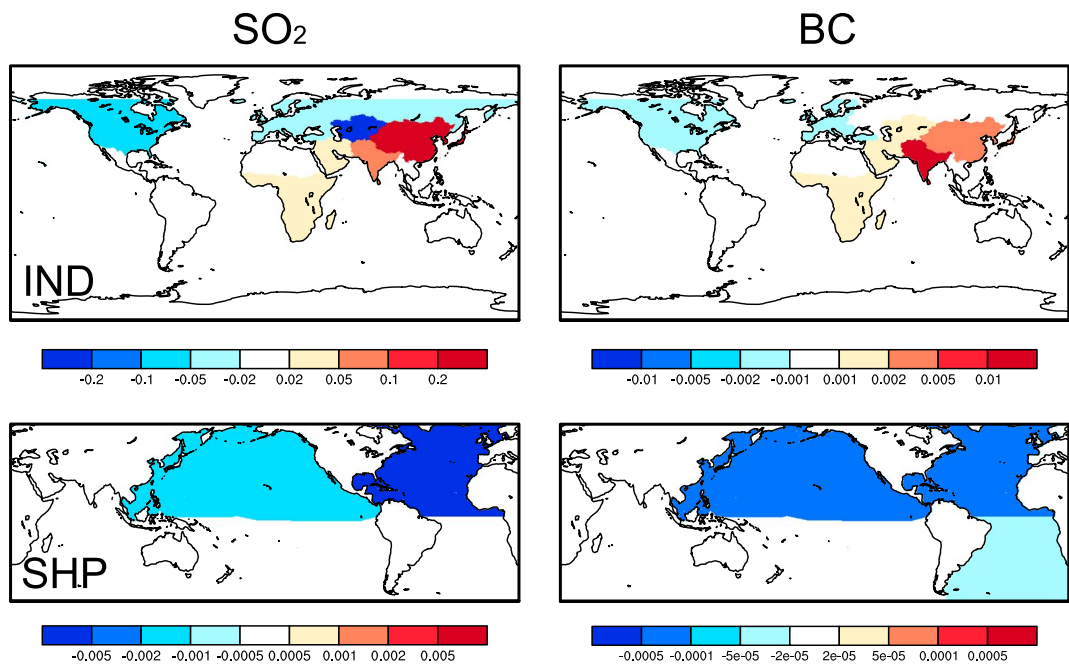


**Figure 9.** Difference in annual mean absolute ranges of near-surface concentrations of  $\text{SO}_2$  (ppbv, left) and black carbon (BC;  $\mu\text{g}/\text{m}^3$ , right) due to the uncertainty in injection heights of industrial (top row) and shipping (bottom row) emissions between the last 5 years and the first 5 years of 2005–2014.

**Table 3**

*Annual Mean Ranges of  $\text{SO}_2$  (ppbv) and BC ( $\mu\text{g}/\text{m}^3$ ) in the First (2005–2009) and Last (2010–2014) 5 Years of 2005–2014 Due to the Uncertainty in Injection Heights of Industrial Emissions, As Well As Their Differences, Over Land Regions Including North America (NAM), Central America (CAM), South America (SAM), Europe (EUR), North Africa (NAF), Southern Africa (SAF), the Middle East (MDE), Southeast Asia (SEA), Central Asia (CAS), South Asia (SAS), East Asia (EAS), Russia/Belarus/Ukraine (RBU, Hereafter Russia), Pacific/Australia/New Zealand (PAN, Hereafter Australia), and Arctic (ARC)*

Year	Range of $\text{SO}_2$ (ppbv)						
	NAM	CAM	SAM	EUR	NAF	SAF	MDE
2005–2009	1.38E–01	6.24E–02	1.41E–01	2.13E–01	3.09E–02	5.88E–02	3.70E–01
2010–2014	8.44E–02	7.06E–02	1.44E–01	1.66E–01	3.06E–02	9.21E–02	4.10E–01
Difference	−5.40E–02	8.21E–03	3.53E–03	−4.67E–02	−3.05E–04	3.32E–02	4.00E–02
	SEA	CAS	SAS	EAS	RBU	PAN	ARC
2005–2009	6.53E–02	7.58E–01	6.69E–01	1.28E+00	2.54E–01	6.43E–02	1.49E–01
2010–2014	4.87E–02	3.88E–01	7.32E–01	1.56E+00	2.34E–01	6.11E–02	1.64E–01
Difference	−1.66E–02	−3.70E–01	6.27E–02	2.76E–s01	−2.07E–02	−3.21E–03	1.46E–02
Range of BC ( $\mu\text{g}/\text{m}^3$ )							
Year	NAM	CAM	SAM	EUR	NAF	SAF	MDE
2005–2009	6.83E–03	3.38E–03	7.96E–03	9.58E–03	1.70E–03	2.85E–03	1.25E–02
2010–2014	5.69E–03	3.44E–03	8.58E–03	8.19E–03	1.79E–03	4.05E–03	1.39E–02
Difference	−1.14E–03	6.70E–05	6.21E–04	−1.39E–03	9.42E–05	1.20E–03	1.39E–03
	SEA	CAS	SAS	EAS	RBU	PAN	ARC
2005–2009	1.22E–02	6.38E–03	6.21E–02	4.95E–02	1.50E–03	8.98E–04	3.64E–05
2010–2014	1.22E–02	7.75E–03	7.87E–02	5.35E–02	1.58E–03	1.15E–03	4.50E–05
Difference	−4.87E–05	1.38E–03	1.66E–02	3.99E–03	8.43E–05	2.48E–04	8.61E–06

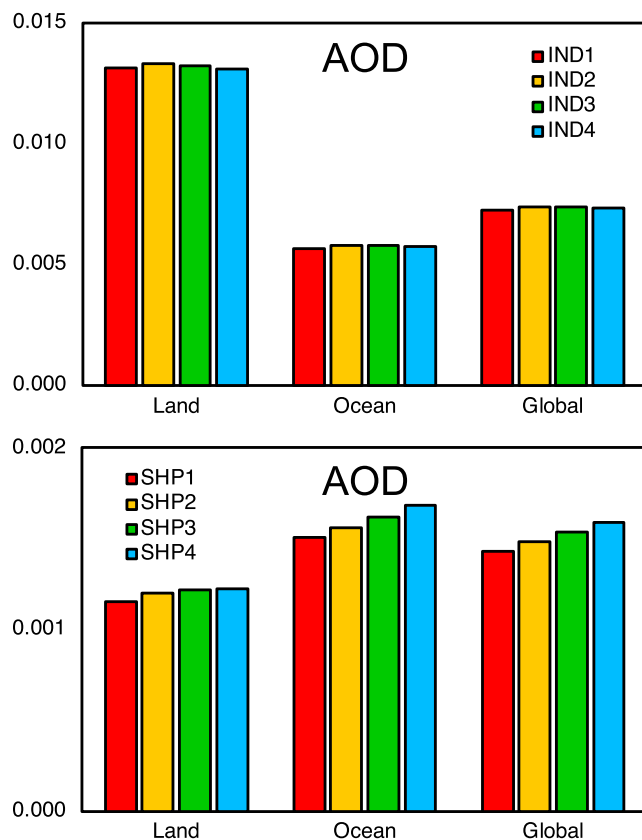


**Figure 10.** Annual mean AOD (aerosol optical depth) of sulfate, black carbon, and primary organic matter over land, oceans, and the whole globe from industrial (top) and shipping (bottom) emissions injected into layer 1 to 4.

Figure 10 shows the annual mean AOD (aerosol optical depth) of sulfate, BC, and POM from industrial and shipping emissions injected into layers 1 to 4. Although the uncertainty in industrial emission height strongly affects concentration and vertical profile of BC and POM, the total AOD from industrial emissions is barely changed, with relative range of AOD within 2% over both land and ocean regions. However, due to less wet removal, shipping emissions with higher injection height give higher AOD, with relative range of AOD of 6% and 11% over land and oceans, respectively. These indicate that the uncertainty in assumed effective emission height not only influences aerosol concentration and vertical profile but also is important to aerosol radiative forcing and its climatic effects, especially for emissions from ocean regions.

#### 4. Conclusion

The few previous studies that have examined the impact of emission injection height have largely focused on natural emissions, for example, open biomass burning and volcanic emissions, or anthropogenic emissions in a specific land region. Using a 10-year (2005–2014) global CAM5 simulation, we find that the injection height uncertainty can influence SO<sub>2</sub> annual global mean near-surface concentration over land (ocean) from industrial (shipping) emissions by 81% (76%). Industrial emission height uncertainty produces variations in modeled near-surface SO<sub>2</sub> concentrations between 70% and 130% over most land regions. Shipping injection height uncertainty produces variations in modeled near-surface SO<sub>2</sub> concentrations of 79%–84% over Northern Hemisphere oceans and 59%–72% over Southern Hemisphere oceans. The influence of emission injection height uncertainty on modeled SO<sub>2</sub> near-surface concentrations is much larger than the overall uncertainty of SO<sub>2</sub> emission rates (estimated to be 8%–14% globally and ~30% in China by Smith et al., 2011). BC and POM concentration and profiles are also sensitive to emission heights (53% over land and 28% over oceans). The uncertainty in shipping emission height also leads to relative ranges of AOD of 6% and 11% over land and oceans, respectively, indicating that the uncertainty in assumed effective emission height not only influences aerosol concentration and vertical profile but also is important to aerosol radiative forcing and its climatic effects, especially for emissions from ocean regions.

#### 5. Discussion

The ranges in this study are comparable to or larger than the range of results across models for most of the aerosol metrics examined by Textor et al. (2006), highlighting the importance of emission height on SO<sub>2</sub> concentrations. The wide variety of industrial sources with varying stack heights and emission characteristics (temperature and exhaust velocity) introduces a significant uncertainty in emission heights for the industrial sector. While power plants and metal smelters with tall stacks are generally important sources, we note that stack height is not always known, particularly in rapidly industrializing regions, and plume rise is not considered in current global models. This means that emission height uncertainties will also be present for these sectors as well.

We show here that emission height has a very large, approximately a factor of 2, impact on surface SO<sub>2</sub> concentration results. This means that without accurate injection height information, attempts to constrain model results using SO<sub>2</sub> observations will be biased. Further, different emission height assumptions in various models will lead to additional, unaccounted for differences in model results that will confound comparisons.

These results also have implications for satellite observations of sulfur dioxide (He et al., 2012, McLinden et al. 2016), which are increasingly being compared to model results. Uncertainty in emissions height will

impact the accuracy of satellite retrievals, since satellite column SO<sub>2</sub> retrievals depend on the assumed vertical distribution of SO<sub>2</sub> in the retrieval algorithm. Because satellite sensors are less sensitive to concentrations in the lower atmosphere, the uncertainty due to incomplete knowledge of emission height will translate to an additional, and as of yet, unquantified uncertainty in satellite retrieval results, particularly for SO<sub>2</sub>. This may be a factor in the model-satellite SO<sub>2</sub> discrepancy seen in China by Yang, Wang, Smith, Easter, et al. (2017) and Yang, Wang, Smith, Easter, and Rasch (2018).

While stack height data are in some regional inventories, this information is not yet part of global emission data sets. Improved data for emission heights, and perhaps a plume rise parameterization suitable for global models, would be needed to reduce the impact of this uncertainty. Uncertainties related to SO<sub>2</sub> oxidation, scavenging, and model parameterizations may also lead to biases in SO<sub>2</sub> and sulfate. These model processes inevitably also dependent upon emission heights. Comparisons of model result to SO<sub>2</sub> observations, therefore, require accurate assumptions for injection height.

We also find a significant emissions height impact for primary aerosol emissions (BC, POM), but the majority of these emissions in most regions are from surface sources (i.e., road transportation and residential combustion), and the injection height of elevated BC and POM emissions is likely to have a smaller impact on biases in total concentration, compared to uncertainty in emission intensity. The primary emissions-related uncertainty for BC and POM in most regions is, therefore, likely to be uncertainty in emissions strength, although there may be regions with large industrial sources of primary aerosol emissions, such as coke ovens, where emission height could be very important.

The results in this study are based on a single climate model whose model resolution is rather coarse compared to the size of plumes from industrial sectors. The uncertainty range calculated in this study could be model dependent. We also note that oxidant fields are fixed as exogenous inputs, which may impact results. It would be very useful to perform an intercomparison between multiple models and/or resolutions, particularly given the diversity in model dispersion magnitude found by Textor et al. (2006). While the influence of emission height on sulfate concentrations, and therefore radiative forcing, was small in this work, this result might not hold for other models. Results would likely depend upon the oxidation, scavenging, and transport rates of the particular model. Further, plume rise is dependent on a combination of stack effluent characteristics and ambient meteorological conditions. Exploration of which would benefit from the application of more spatially detailed modeling. Also, the simulation performed here lacks nitrate chemistry, the inclusion of which could also influence the ranges of SO<sub>2</sub> and sulfate.

#### Acknowledgments

This research was support by the National Aeronautics and Space Administration's Atmospheric Composition: Modeling and Analysis Program (ACMAP) award NNN15AZ64I and by the U.S. Department of Energy (DOE), Office of Science, Biological and Environmental Research. The Pacific Northwest National Laboratory is operated for DOE by Battelle Memorial Institute under contract DE-AC05-76RLO1830. The National Energy Research Scientific Computing Center (NERSC) provided computational support. All the data used are archived at [http://portal.nersc.gov/project/m1374/Injection\\_Height/](http://portal.nersc.gov/project/m1374/Injection_Height/).

#### References

- Akingunola, A., Makar, P. A., Zhang, J., Darlington, A., Li, S.-M., Gordon, M., et al. (2018). A chemical transport model study of plume-rise and particle size distribution for the Athabasca oil sands. *Atmospheric Chemistry and Physics*, 18, 8667–8688. <https://doi.org/10.5194/acp-18-8667-2018>
- Bieser, J., Aulinger, A., Matthias, V., Quante, M., & Denier van der Gon, H. A. C. (2011). Vertical emission profiles for Europe based on plume rise calculations. *Environmental Pollution*, 159, 2935–2946. <https://doi.org/10.1016/j.envpol.2011.04.030>
- Carson, J. E., & Moses, H. (1969). Validity of several plume rise formulas. *Journal of the Air Pollution Control Association*, 19, 862–866. <https://doi.org/10.1080/00022470.1969.10469350>
- de Meij, A., Krol, M., Dentener, F., Vignati, E., Cuvelier, C., & Thunis, P. (2006). The sensitivity of aerosol in Europe to two different emission inventories and temporal distribution of emissions. *Atmospheric Chemistry and Physics*, 6, 4287–4309. <https://doi.org/10.5194/acp-6-4287-2006>
- Dentener, F., Kinne, S., Bond, T., Boucher, O., Cofala, J., Generoso, S., et al. (2006). Emissions of primary aerosol and precursor gases in the years 2000 and 1750 prescribed data-sets for AeroCom. *Atmospheric Chemistry and Physics*, 6, 4321–4344. <https://doi.org/10.5194/acp-6-4321-2006>
- Ge, C., Wang, J., Carn, S., Yang, K., Ginoux, P., & Krotkov, N. (2016). Satellite-based global volcanic SO<sub>2</sub> emissions and sulfate direct radiative forcing during 2005–2012. *Journal of Geophysical Research: Atmospheres*, 121, 3446–3464. <https://doi.org/10.1002/2015JD023134>
- Gordon, M., Makar, P. A., Staebler, R. M., Zhang, J., Akingunola, A., Gong, W., & Li, S.-M. (2017). A comparison of plume rise algorithms to stack plume measurements in the athabasca oil sands. *Atmospheric Chemistry and Physics Discussions*, in review. <https://doi.org/10.5194/acp-2017-1093>
- Guevara, M., Soret, A., Arévalo, G., Martínez, F., & Baldasano, J. M. (2014). Implementation of plume rise and its impacts on emissions and air quality modelling. *Atmospheric Environment*, 99, 618–629. <https://doi.org/10.1016/j.atmosenv.2014.10.029>
- He, H., Li, C., Loughner, C. P., Li, Z., Krotkov, N. A., Yang, K., et al. (2012). SO<sub>2</sub> over central China: Measurements, numerical simulations and the tropospheric sulfur budget. *Journal of Geophysical Research*, 117, D00K37. <https://doi.org/10.1029/2011JD016473>
- Hoesly, R. M., Smith, S. J., Feng, L., Klimont, Z., Janssens-Maenhout, G., Pitkanen, T., et al. (2018). Historical (1750–2014) anthropogenic emissions of reactive gases and aerosols from the Community Emissions Data System (CEDS). *Geoscientific Model Development*, 11, 369–408. <https://doi.org/10.5194/gmd-11-369-2018>

- Hurrell, J. W., Holland, M. M., Gent, P. R., Ghan, S., Kay, J. E., Kushner, P. J., et al. (2013). The Community Earth System Model A Framework for collaborative research. *Bulletin of The American Meteorological Society*, 94, 1339–1360. <https://doi.org/10.1175/BAMS-D-12-00121.1>
- Jian, Y., & Fu, T.-M. (2014). Injection heights of springtime biomass-burning plumes over peninsular Southeast Asia and their impacts on long-range pollutant transport. *Atmospheric Chemistry and Physics*, 14, 3977–3989. <https://doi.org/10.5194/acp-14-3977-2014>
- Li, C., McLinden, C., Fioletov, V., Krotkov, N., Carn, S., Joiner, J., et al. (2017). India is overtaking China as the world's largest emitter of anthropogenic sulfur dioxide. *Scientific Reports*, 7, 14304. <https://doi.org/10.1038/s41598-017-14639-8>
- Liu, X., Easter, R. C., Ghan, S. J., Zaveri, R., Rasch, P., Shi, X., et al. (2012). Toward a minimal representation of aerosols in climate models: description and evaluation in the Community Atmosphere Model CAM5. *Geoscientific Model Development*, 5, 709–739. <https://doi.org/10.5194/gmd-5-709-2012>
- Luderer, G., Trentmann, J., Winterrath, T., Textor, C., Herzog, M., Graf, H.-F., & Andreae, M. (2006). Modeling of biomass smoke injection into lower stratosphere by a large forest fire: Sensitivity studies. *Atmospheric Chemistry and Physics*, 6, 5261–5277. <https://doi.org/10.5194/acp-6-5261-2006>
- Mailler, S., Khorostyanov, D., & Menut, L. (2013). Impact of the vertical emission profiles on background gas-phase pollution simulated from the EMEP emissions over Europe. *Atmospheric Chemistry and Physics*, 13, 5987–5998. <https://doi.org/10.5194/acp-13-5987-2013>
- McLinden, C. A., Fioletov, V., Shephard, M. W., Krotkov, N., Li, C., Martin, R. V., et al. (2016). Space-based detection of missing sulfur dioxide sources of global air pollution. *Nature Geoscience*, 9, 496–500. <https://doi.org/10.1038/ngeo2724>
- Myhre, G., Samsen, B. H., Schulz, M., Balkanski, Y., Bauer, S., Berntsen, T. K., et al. (2013). Radiative forcing of the direct aerosol effect from AeroCom Phase II simulations. *Atmospheric Chemistry and Physics*, 13, 1853–1877. <https://doi.org/10.5194/acp-13-1853-2013>
- Pozzer, A., Jöckel, P., & Van Aardenne, J. (2009). The influence of the vertical distribution of emissions on tropospheric chemistry. *Atmospheric Chemistry and Physics*, 9, 9417–9432. <https://doi.org/10.5194/acp-9-9417-2009>
- Pregger, T., & Friedrich, R. (2009). Effective pollutant emission heights for atmospheric transport modelling based on real-world information. *Environmental Pollution*, 157(2), 552–560. <https://doi.org/10.1016/j.envpol.2008.09.027>
- Rienecker, M. M., Suarez, M. J., Gelaro, R., Todling, R., Bacmeister, J., Liu, R., et al. (2011). MERRA: NASA's Modern-Era Retrospective Analysis for Research and Applications. *Journal of Climate*, 24, 3624–3648. <https://doi.org/10.1175/JCLI-D-11-00015.1>
- Roelofs, G. J., Kasibhatla, P., Barrie, L., Bergmann, D., Bridgeman, C., Chin, M., et al. (2001). Analysis of regional budgets of sulfur species modeled for the COSAM exercise. *Tellus B*, 53, 673–694. <https://doi.org/10.1034/j.1600-0889.2001.530509.x>
- Smith, S. J., van Aardenne, J., Klimont, Z., Andres, R. J., Volke, A., & Delgado Arias, S. (2011). Anthropogenic sulfur dioxide emissions: 1850–2005. *Atmospheric Chemistry and Physics*, 11, 1101–1116. <https://doi.org/10.5194/acp-11-1101-2011>
- Sofiev, M., Vankevich, R., Ermakova, T., & Hakkarainen, J. (2013). Global mapping of maximum emission heights and resulting vertical profiles of wildfire emissions. *Atmospheric Chemistry and Physics*, 13, 7039–7052. <https://doi.org/10.5194/acp-13-7039-2013>
- Stier, P., Feichter, J., Kinne, S., Kloster, S., Vignati, E., Wilson, J., et al. (2005). The aerosol-climate model ECHAM5-HAM. *Atmospheric Chemistry and Physics*, 5, 1125–1156. <https://doi.org/10.5194/acp-5-1125-2005>
- Textor, C., Schulz, M., Guibert, S., Kinne, S., Balkanski, Y., Bauer, S., et al. (2006). Analysis and quantification of the diversities of aerosol life cycles within AeroCom. *Atmospheric Chemistry and Physics*, 6, 1777–1813. <https://doi.org/10.5194/acp-6-1777-2006>
- Tsigaridis, K., Daskalakis, N., Kanakidou, M., Adams, P. J., Artaxo, P., Bahadur, R., et al. (2014). The AeroCom evaluation and inter-comparison of organic aerosol in global models. *Atmospheric Chemistry and Physics*, 14, 10,845–10,895. <https://doi.org/10.5194/acp-14-10845-2014>
- van Marle, M. J. E., Kloster, S., Magi, B. I., Marlon, J. R., Daniau, A.-L., Field, R. D., et al. (2017). Historic global biomass burning emissions for CMIP6 (BB4CMIP) based on merging satellite observations with proxies and fire models (1750–2015). *Geoscientific Model Development*, 10, 3329–3357. <https://doi.org/10.5194/gmd-10-3329-2017>
- Wang, H., Easter, R. C., Rasch, P. J., Wang, M., Liu, X., Ghan, S. J., et al. (2013). Sensitivity of remote aerosol distributions to representation of cloud-aerosol interactions in a global climate model. *Geoscientific Model Development*, 6, 765–782. <https://doi.org/10.5194/gmd-6-765-2013>
- Yang, Y., Wang, H., Smith, S. J., Easter, R., Ma, P.-L., Qian, Y., et al. (2017). Global source attribution of sulfate concentration and direct and indirect radiative forcing. *Atmospheric Chemistry and Physics*, 17, 8903–8922. <https://doi.org/10.5194/acp-17-8903-2017>
- Yang, Y., Wang, H., Smith, S. J., Easter, R. C., & Rasch, P. J. (2018). Sulfate aerosol in the Arctic: Source attribution and radiative forcing. *Journal of Geophysical Research: Atmospheres*, 123, 1899–1918. <https://doi.org/10.1002/2017JD027298>
- Yang, Y., Wang, H., Smith, S. J., Ma, P.-L., & Rasch, P. J. (2017). Source attribution of black carbon and its direct radiative forcing in China. *Atmospheric Chemistry and Physics*, 17, 4319–4336. <https://doi.org/10.5194/acp-17-4319-2017>
- Yang, Y., Wang, H., Smith, S. J., Zhang, R., Lou, S., Qian, Y., et al. (2018). Recent intensification of winter haze in China linked to foreign emissions and meteorology. *Scientific Reports*, 8, 2107. <https://doi.org/10.1038/s41598-018-20437-7>
- Yang, Y., Wang, H., Smith, S. J., Zhang, R., Lou, S., Yu, H., et al. (2018). Source apportionments of aerosols and their direct radiative forcing and long-term trends over continental United States. *Earth's Future*, 6, 793–808. <https://doi.org/10.1029/2018EF000859>